

THE DYNAMICS OF A STOICHIOMETRIC PLANT-HERBIVORE MODEL AND ITS DISCRETE ANALOG

GUANGYU SUI

School of Mathematics and Statistics, Northeast Normal University
5268 Renmin Street, Changchun, Jilin, 130024, P. R. China

MENG FAN

School of Mathematics and Statistics, KLVE and KLAS, Northeast Normal University
5268 Renmin Street, Changchun, Jilin, 130024, P. R. China

IRAKLI LOLADZE

Department of Mathematics, University of Nebraska-Lincoln, Lincoln, NE 68588

YANG KUANG

Department of Mathematics and Statistics, Arizona State University, Tempe, AZ 85287

ABSTRACT. Stoichiometry-based models brought into sharp focus the importance of the nutritional quality of plant for herbivore-plant dynamics. Plant quality can dramatically affect the growth rate of the herbivores and may even lead to its extinction. These results stem from models continuous in time, which raises the question of how robust they are to time discretization. Discrete time can be more appropriate for herbivores with non-overlapping generations, annual plants, and experimental data collected periodically. We analyze a continuous stoichiometric plant-herbivore model that is mechanistically formulated in [11]. We then introduce its discrete analog and compare the dynamics of the continuous and discrete models. This discrete model includes the discrete LKE model (Loladze, Kuang and Elser (2000)) as a limiting case.

1. Introduction. Mechanistically formulated mathematical models of population dynamics have advantage over phenomenologically derived models in generating plausible and verifiable dynamics. However, the challenge of developing a mechanistic and predictive theory for biological systems is often daunting. Exciting progress in understanding and modeling ecological systems in the last decade has been achieved through the applications of the theory of ecological stoichiometry [22]. *Ecological stoichiometry* is the study of the balance of energy and multiple chemical resources (usually elements) in ecological interactions. It provides rigorous and ubiquitous mechanism for modeling population dynamics. It has been fruitfully deployed in the study of competition for multiple abiotic resources ([23], [8]), producer-grazer systems ([1], [16], [18]), producer-decomposer systems [9], recycling of nutrients by consumers [6], the maintenance of chemical homeostasis by herbivores consuming food that is unbalanced relative to their needs ([13],[14]), and competition among consumers ([17], [10]). When constructing population models,

2000 *Mathematics Subject Classification.* 92D40, 34K20.

Key words and phrases. stoichiometry, plant-herbivore interaction, discrete model, Droop equation, bifurcation.

one often implicitly assumes that all trophic levels are chemically homogeneous or are made of a single constituent that often represents energy. But in the real world, all organisms are composed of many chemical elements such as carbon (C), nitrogen (N), phosphorus (P), and other essential elements. Moreover, the concentrations of essential elements vary considerably among species. If the quantity of an essential element in a plant is lower than the minimum threshold for its consumer, then the consumer's growth rate may suffer. This has been shown for both aquatic ([24],[26],[19]), and terrestrial systems (e.g., ([12])). For example, Newman et al. ([20]) observed that while elevated carbon dioxide benefited host plants, it resulted in smaller populations of the bird cherry-oat aphid *Rhopalosiphum padi*. Loladze ([15]) discusses how elevated carbon dioxide can alter the stoichiometry of crops and affect human nutrition.

Loladze et al. [16] constructed and studied the simplest dynamic stoichiometric predator-prey model (LKE model), which is based on a batch culture experiment ([24]), with different light intensities and the limited amount of one essential element, P. The model showed that overall, food quality, as measured by P content in the producer (prey), had significant impact on the grazer (predator). Specifically, the model showed behavior not seen in the corresponding traditional predator-prey model:

- (1) Extremely low food quality leads to the deterministic extinction of the grazer.
- (2) Two stable equilibria (not necessarily simultaneous) are possible: (A) one with high grazer/producer ratio at the high food quality, and (B) one with low grazer/producer ratio at the low food quality.
- (3) The enrichment of the system, as measured by the intensity of light, can abruptly halt producer-grazer oscillations; the system settles at an equilibrium with low grazer/producer ratio.

Are these dynamics simply the artifacts of the particular structure and assumptions of the model, or are they the valid outcomes of bringing stoichiometric realities into predator-prey dynamics? One way to answer these questions is to analyze a family of models that share stoichiometric underpinning, but differ in their mathematical structure or assumptions. If a phenomenon is present across the family of models, it gives assurance of its robustness. This approach can provide an additional benefit. The mathematical structure of the Loladze et al. [16] model (a two-dimensional autonomous ODE system) precludes a possibility for chaos. However, Andersen (1997) suggested chaotic dynamics in his higher-dimensional stoichiometric model. If mathematical restriction on chaos is removed, can chaotic dynamics arise in a low-dimensional stoichiometric producer-grazer system? For example, discretizing continuous in time system lifts such a restriction because a discrete system consisting of just one equation can potentially exhibit chaos.

To answer the above questions, we compare the dynamics of four stoichiometric models: two continuous models and their two discrete analogs. The continuous LKE model assumes immediate recycling of P from excreted and dead matter and instantaneous P uptake by the producer. While this model provides a qualitatively good match to experimental data ([25]), it nevertheless raises the question of the robustness of the results to such an assumption. A potentially substantial pool of free P exists in many real systems. Although the concentration of free P is very low in nutrient-limited pelagic systems, it is unlikely to be so for terrestrial systems. Kuang et al. [11] introduced a simple and mathematically tractable continuous model (KHE model) that provides a slightly more mechanistic formulation of the

dynamics of some plant-herbivore interactions in P-limited environment. It incorporates the LKE model in [16] as a special case. The model's derivation is based on the Droop equation and without the hypothesis of immediate recycling of P. That is, there exists free P in the system. The study in [11] reveals that the details in ecological stoichiometry models matter for quantitative predictions of plant-herbivore dynamics, especially at intermediate ranges of the carrying capacity. This interesting conclusion is based purely on numerical simulations.

Both stoichiometric models mentioned above are continuous in time. However, experimental data are usually collected on discrete time intervals, many plants in wild and agricultural settings have non-overlapping generations, and many herbivores have clear annual or seasonal dynamics. Such scenarios call for discrete models. This raises the question about the sensitivity of the results to the discretization of time. Fan et al. [7] compared the continuous stoichiometric LKE producer-grazer model to its discrete analog both theoretically and numerically. They show that in continuous models and in discrete models, the stoichiometric effects of producer quality on grazers are similar. In this paper, we study analytically and numerically the dynamics of the continuous KHE plant-herbivore model and its discrete analogue. In addition, we compare the findings in [7] with ours. This allows us to compare the robustness of stoichiometric results in four models: the LKE, the KHE, and their discrete analogs. We show that all three stoichiometric effects listed above are present in all four models. In addition, we show that discretizing either of the continuous systems allows for chaotic dynamics within the biologically meaningful range of parameter values. Section 2 focuses on the qualitative analysis of the continuous KHE plant-herbivore model in [11]. Then, in Section 3, we will investigate the dynamics of its discrete analogue and compare their dynamics. In Section 4, we will systematically discuss the similarities and the differences of the four models.

2. The continuous KHE model. We introduce the continuous plant-herbivore model established in [11], which is called the KHE model in this paper for convenience and simplicity.

Assume the following:

(A₁) The total mass of phosphorus in the entire system is fixed; i.e., the system is closed for phosphorus.

(A₂) Phosphorus to carbon ratio(P:C) in the plant varies, but it never falls below a minimum; the herbivore maintains a constant P:C ratio.

(A₃) The phosphorus in the system is divided into three pools: phosphorus in plant, phosphorus in herbivore, and free phosphorus.

Based on these assumptions, and with the help of a variable-internal-stores model based on the Droop equation relating growth rate to the internal cell quota ([3]), Kuang et al. [11] proposed the following continuous stoichiometric plant-herbivore model:

$$\begin{aligned} \frac{dx}{dt} &= bx \left[1 - \max \left(\frac{x}{K}, \frac{x + \mu_m \alpha^{-1}}{[b/\mu_m][\mu_m \alpha^{-1} + (P_t - \theta y)/q]} \right) \right] - f(x)y, \\ \frac{dy}{dt} &= e \min(1, \frac{Q}{\theta}) f(x)y - dy. \end{aligned} \quad (2.1)$$

TABLE 1. A sample set of parameters and their biological meaning in (2.1).

Parameters	Biological definition
x	the density of plant (mg C/l)
y	the density of herbivore (mg C/l)
$b = \mu_m - D$	the intrinsic growth rate of plant (day^{-1})
d	the specific loss rate of herbivore (day^{-1})
e	a constant production efficiency (yield constant)
K	the plant's carrying capacity depending on other factors
q	the minimum P:C ratio in the plant (mg P/mg C)
μ_m	the plant's true maximal growth rate
D	the plant's death rate
Q	the plants cell quota for P
α	nutrient recruitment rate
θ	the herbivore maintains a constant P:C ratio ((mg P/mg C))
$f(x)$	the herbivore's ingestion rate
P_t	the total mass of phosphorus in the entire system
P_p	the phosphorus in plant
P_z	the phosphorus in herbivore
P_f	the free phosphorus

Here

$$P_t = P_p + P_z + P_f, \quad Q = q + \frac{\alpha}{\mu_m + \alpha x}(P_t - qx - \theta y). \quad (2.2)$$

A sample set of parameters in (2.1) and their biological meanings are listed in Table 1.

In the following, we assume that $f(x)$ in (2.1) is a bounded smooth function satisfying

$$f(x) = xp(x), \quad f(0) = 0, \quad f'(x) > 0, \quad f'(0) < \infty, \quad f''(x) < 0, \quad x > 0.$$

Then, from [16] (Appendix A), it follows that for any $x > 0$,

$$\limsup_{x \rightarrow 0} p(x) = f'(0) < \infty, \quad p'(x) < 0.$$

First we state a theorem on the boundedness and postivie invariance of the solutions of (2.1). The proof is very similar to those in [16] (Appendix C), so the details are omitted here.

THEOREM 2.1. *Solutions with initial conditions in the open trapezoid (or triangle if $K > P_t/q$)*

$$\Delta \equiv \{(x, y) : 0 < x < k, 0 < y, qx + \theta y < P_t\} \quad (2.3)$$

remain there for all forward times, where

$$k = \min(K, P_t/q). \quad (2.4)$$

We use $\bar{\Delta}$ to denote the region Δ together with its boundary with the exception of $(0, P_t/\theta)$ (which is biologically insignificant because at this point the herbivore

contains all phosphorus and plant is absent from the system). In other words,

$$\bar{\Delta} = (\partial\Delta/(0, P_t/\theta)) \cup \Delta. \quad (2.5)$$

For convenience, we rewrite (2.1) in the following form:

$$\frac{dx}{dt} = xF(x, y), \quad \frac{dy}{dt} = yG(x, y), \quad (2.6)$$

where

$$\begin{aligned} F(x, y) &= b \left[1 - \max \left(\frac{x}{K}, \frac{x + \mu_m \alpha^{-1}}{[b/\mu_m][\mu_m \alpha^{-1} + (P_t - \theta y)/q]} \right) \right] - \frac{f(x)}{x} y, \\ G(x, y) &= e \min \left(1, \frac{Q}{\theta} \right) f(x) - d. \end{aligned} \quad (2.7)$$

In the following, we let

$$\begin{aligned} A(x) &\equiv \left(\frac{-\mu_m(Kx + K\mu_m \alpha^{-1})}{xb} + \mu_m \alpha^{-1} + \frac{P_t}{q} \right) \frac{q}{\theta}, \\ B(x) &\equiv P_t/\theta - (x + \mu_m/\alpha - q\mu_m/\alpha\theta). \end{aligned}$$

After some trivial algebraic calculations, the partial derivatives of F and G read

$$\begin{aligned} F_x &= -b \max \left(\frac{1}{K}, \frac{1}{[b/\mu_m][\mu_m \alpha^{-1} + (P_t - \theta y)/q]} \right) - \left(\frac{f(x)}{x} \right)' y, \\ F_y &= \begin{cases} -p(x), & y < A(x), \\ -\frac{\mu_m \theta (x + \mu_m \alpha^{-1})}{q(\mu_m \alpha^{-1} + (P_t - \theta y)/q)^2} - p(x), & y > A(x), \end{cases} \\ G_x &= \begin{cases} e[p(x) + xp'(x)], & y < B(x), \\ \frac{e(P_t - \theta y + \mu_m q \alpha^{-1})}{\theta(\mu_m \alpha^{-1} + x)^2} (f'(x)(\mu_m \alpha^{-1} + x) - f(x)), & y > B(x), \end{cases} \\ G_y &= \begin{cases} 0, & y < B(x), \\ -\frac{x \cdot e \cdot p(x)}{\mu_m \alpha^{-1} + x}, & y > B(x). \end{cases} \end{aligned} \quad (2.8)$$

The equilibria of (2.1) solve the algebraic equations $xF(x, y) = 0$, $yG(x, y) = 0$. It is easy to see that the boundary equilibria of (2.1) are $E_0 = (0, 0)$ and $E_1 = (k, 0)$. To determine the local stability of these equilibria, we calculate the Jacobian of (2.1),

$$J(x, y) = \begin{pmatrix} F(x, y) + xF_x(x, y) & xF_y(x, y) \\ yG_x(x, y) & G(x, y) + yG_y(x, y) \end{pmatrix}. \quad (2.9)$$

THEOREM 2.2. $E_0 = (0, 0)$ is always a saddle. For $E_1 = (k, 0)$, if $G(k, 0) > 0$, then it is a saddle; if $G(k, 0) < 0$, then it is locally asymptotically stable (LAS).

Proof. The conclusions directly follow from the fact that

$$J(E_0) = \begin{pmatrix} b \left(1 - \frac{\mu_m^2 \alpha^{-1}}{b(\mu_m \alpha^{-1} + P_t/q)} \right) & 0 \\ 0 & -d \end{pmatrix}, \quad J(E_1) = \begin{pmatrix} -b & kF_y(k, 0) \\ 0 & G(k, 0) \end{pmatrix}. \quad \blacksquare$$

REMARK 1. We cannot determine the sign of G_x when $Q < \theta$, so we cannot use the intermediate value theorem to determine the solutions of $G(x, y) = 0$ or restrict the range of the boundary equilibria stability as in [16].

Now we turn to the LAS of the internal equilibrium of (2.1). Note that $-(F_x/F_y)$ and $-(G_x/G_y)$ represent the slopes of the plant and herbivore nullclines at (x, y) , respectively. Suppose that $E^*(x^*, y^*)$ is one such equilibrium; i.e., $F(x^*, y^*) = 0$ and $G(x^*, y^*) = 0$. The Jacobian at E^* is

$$J(x^*, y^*) = \begin{pmatrix} x^* F_x(x^*, y^*) & x^* F_y(x^*, y^*) \\ y^* G_x(x^*, y^*) & y^* G_y(x^*, y^*) \end{pmatrix},$$

and its determinant and trace are

$$\text{Det}(J(x^*, y^*)) = x^* y^* (F_x G_y - F_y G_x), \quad (2.10)$$

$$\text{Tr}(J(x^*, y^*)) = x^* F_x + y^* G_y. \quad (2.11)$$

Let

$$\begin{aligned} \Omega_1 &= \{(x, y) : x > 0, y > 0, y < P_t/\theta - (x + \mu_m/\alpha - q\mu_m/\alpha\theta)\}, \\ \Omega_2 &= \{(x, y) : x > 0, y > 0, y > P_t/\theta - (x + \mu_m/\alpha - q\mu_m/\alpha\theta)\}. \end{aligned}$$

Notice that Ω_1 and Ω_2 are the regions in the positive cone separated by the line $y = -x + P_t/\theta - \mu_m/\alpha + q\mu_m/\alpha\theta$.

THEOREM 2.3. *In region Ω_1 , if the plant nullcline is decreasing at E^* , then E^* is LAS; if the plant nullcline is increasing at E^* , then E^* is a repeller. In region Ω_2 , if $-G_x/G_y < -F_x/F_y$, then E^* is a saddle; if $(\ln f(x^*))'(\mu_m\alpha^{-1} + x^*) - 1 < 0$ and $-G_x/G_y > -F_x/F_y$, then E^* is LAS.*

Proof. Suppose that $E^* \in \Omega_1$, then (2.8) yields that $F_y < 0, G_x > 0, G_y = 0$ at (x^*, y^*) . Hence, $\text{Det}(J(x^*, y^*)) > 0$. Moreover,

$$\text{sign}(\text{Tr}(J(x^*, y^*))) = \text{sign}(F_x) = \text{sign}\left(-\frac{F_x}{F_y}\right).$$

If the plant nullcline declines at E^* (i.e., $-F_x/F_y < 0$), then $\text{Tr}(J(x^*, y^*)) < 0$, and hence E^* is LAS. If the plant nullcline at E^* is increasing, then E^* is a repeller.

Suppose that $E^* \in \Omega_2$; then (2.8) implies that at E^* , $F_y < 0, G_y < 0$. Then

$$\text{sign}(\text{Det}(J)) = \text{sign}(F_x G_y - F_y G_x) = \text{sign}\left(\frac{F_x G_y - F_y G_x}{F_y G_y}\right) = \text{sign}\left(-\frac{G_x}{G_y} - \left(-\frac{F_x}{F_y}\right)\right).$$

If $-G_x/G_y < -F_x/F_y$, i.e., the slope of the plant nullcline at E^* is greater than that of the herbivore, then (2.10) is negative. So we can claim that E^* is a saddle. If $-G_x/G_y > -F_x/F_y$ (i.e., the herbivore nullcline at (x^*, y^*) is greater than that of the plant), then (2.10) is positive. Moreover, if $(\ln f(x^*))'(\mu_m\alpha^{-1} + x^*) - 1 < 0$, we have $G_x < 0$. Then

$$0 > -\frac{G_x}{G_y} > -\frac{F_x}{F_y},$$

which, together with $F_y < 0$, implies that $F_x < 0$. Therefore, $\text{Tr}(J(x^*, y^*)) < 0$, and E^* is LAS. \blacksquare

REMARK 2. If $(\ln f(x^*))'(\mu_m\alpha^{-1} + x^*) - 1 > 0$, then $G_x > 0$. In this case, we cannot determine the sign of F_x directly. Hence, we cannot obtain the sign of $\text{Tr}(J(x^*, y^*))$ unless we can choose some interval of x which helps us determine the sign of $\text{Tr}(J(x^*, y^*))$.

REMARK 3. In [16], the authors establish exactly the same criteria for the LKE model, except for the second case in region Ω_2 . For the LKE model, $G_x < 0$ implies the LAS of internal equilibrium. But here, the situation is more complex and difficult.

3. The discrete KHE model. In this section, we consider the discrete analogue of the continuous KHE model (2.1). There are several ways of deriving discrete time versions of dynamical systems corresponding to a continuous time formulation. Here we follow the method used in [7].

Assume that the per capita growth rates in (2.1) change only at a $t = 0, 1, 2, \dots$; then

$$\begin{aligned} \frac{1}{x(t)} \frac{dx(t)}{dt} &= b \left[1 - \max \left(\frac{x([t])}{K}, \frac{x([t]) + \mu_m \alpha^{-1}}{\frac{b}{\mu_m} \left(\frac{\mu_m}{\alpha} + \frac{(P_t - \theta y([t]))}{q} \right)} \right) \right] - \frac{f(x([t])y([t]))}{x([t])}, \\ \frac{1}{y(t)} \frac{dy(t)}{dt} &= e \min \left(1, \frac{Q([t])}{\theta} \right) f(x([t])) - d, t \neq 0, 1, 2, \dots \end{aligned} \quad (3.1)$$

Here $[t]$ denotes the integer part of $t \in (0, +\infty)$. Let

$$C(n) \equiv \frac{b}{\mu_m} \left(\mu_m \alpha^{-1} + \frac{(P_n - \theta y(n))}{q} \right).$$

On any interval $[n, n+1)$, $n = 0, 1, 2, \dots$, we can integrate (3.1) and obtain the following equations for $n \leq t < n+1$:

$$\begin{aligned} x(t) &= x(n) \exp \left\{ \left[b \left[1 - \max \left(\frac{x(n)}{K}, \frac{x(n) + \mu_m \alpha^{-1}}{C(n)} \right) \right] - \frac{f(x(n))y(n)}{x(n)} \right] (t-n) \right\}, \\ y(t) &= y(n) \exp \left\{ \left[e \min \left(1, \frac{Q(n)}{\theta} \right) f(x(n)) - d \right] (t-n) \right\}. \end{aligned}$$

Letting $t \rightarrow n+1$ gives

$$\begin{aligned} x(n+1) &= x(n) \exp \left\{ b \left[1 - \max \left(\frac{x(n)}{K}, \frac{x(n) + \mu_m \alpha^{-1}}{C(n)} \right) \right] - \frac{f(x(n))y(n)}{x(n)} \right\}, \\ y(n+1) &= y(n) \exp \left\{ e \min \left(1, \frac{Q(n)}{\theta} \right) f(x(n)) - d \right\}, \end{aligned} \quad (3.2)$$

which is a discrete time analogue of (2.1). In this section, we focus our attention on the dynamics of (3.2). Considering the biological significance of (3.2), we assume that $x(0) > 0$ and $P/\theta > y(0) > 0$.

Note, that (3.2) incorporates the discrete LKE model [7] as a limiting case. We use the same assumption in [11], in which it is proved that the LKE model

$$\begin{aligned} \frac{dx}{dt} &= bx \left[1 - \frac{x}{\min(K, (P - \theta y)/q)} \right] - f(x)y, \\ \frac{dy}{dt} &= e \min \left(1, \frac{P - \theta y}{\theta x} \right) f(x)y - dy \end{aligned} \quad (3.3)$$

is a limiting case of (2.1). One key difference between the LKE model and the KHE model is that, in the LKE model, all phosphorus is divided into two pools: phosphorus in the herbivore and phosphorus in the plant. That is, there is no freely available phosphorus in the system ($P_f = 0$). This is equivalent to $\alpha = \infty$ or $\alpha^{-1} = 0$. In addition, we assume that the plant death rate D is extremely small compared to μ_m . One may approximate the value of $b/\mu_m = (\mu_m - D)/\mu_m \approx 1$, then

(3.2) reduces to

$$\begin{aligned} x(n+1) &= x(n) \exp \left\{ (b - b \max \left(\frac{x(n)}{K}, \frac{x(n)}{(P_t - \theta y(n))/q} \right) - \frac{f(x(n))y(n)}{x(n)}) \right\}, \\ y(n+1) &= y(n) \exp \left\{ e \min \left(1, \frac{Q(n)}{\theta} \right) f(x(n)) - d \right\}. \end{aligned} \quad (3.4)$$

From equation (2.2), we can get the discrete form of Q

$$Q(n) = \frac{1}{\mu_m \alpha^{-1} + x(n)} (P_t - \theta y(n) + \mu_m q \alpha^{-1}).$$

Hence, as α tends to ∞ , Q tends to $(P_t - \theta y(n))/x(n)$. So, when there is no free phosphorus in the system, the discrete KHE model reduces to the discrete LKE model proposed and investigated in [7],

$$\begin{aligned} x(n+1) &= x(n) \exp \left\{ b \left[1 - \max \left(\frac{x(n)}{K}, \frac{qx(n)}{P_t - \theta y(n)} \right) \right] - \frac{f(x(n))y(n)}{x(n)} \right\}, \\ y(n+1) &= y(n) \exp \left\{ e \min \left(1, \frac{P_t - \theta y(n)}{\theta x(n)} \right) f(x(n)) - d \right\}. \end{aligned} \quad (3.5)$$

First, we prove some preliminary results for (3.2), such as boundedness and positive invariance. It is easy to see that both components of the solution of (3.2) stay positive when they exist. By carrying out arguments like those in Theorems 3.1 and 3.2 in [7], we reach the following theorem.

THEOREM 3.1. *For (3.2), we have*

$$x(n) \leq \max \left\{ x(0), \frac{K}{b} \exp \{ b - 1 \} \right\} := U, \quad y(n) \leq \max \{ y(0), v \} \exp \{ 2ef(U) - 2d \},$$

where v is any number satisfying $ef(U \exp \{ b - p(U)v \}) < d$. In addition,

$$\Delta = \left\{ (x, y) : 0 < x < \frac{K}{b} \exp \{ b - 1 \}, 0 < y < v \right\}$$

is positively invariant and Δ is globally attractive with respect to initial values $(x(0), y(0))$ such that $x(0) > 0$ and $P/\theta > y(0) > 0$.

Next, we focus on analyzing the stability of the equilibria of (3.2). For convenience, we rewrite (3.2) as

$$\begin{aligned} x(n+1) &= x(n) \exp \{ F(x(n), y(n)) \}, \\ y(n+1) &= y(n) \exp \{ G(x(n), y(n)) \}, \end{aligned} \quad (3.6)$$

where

$$\begin{aligned} F(x, y) &= b - b \max \left(\frac{x}{K}, \frac{x + \mu_m \alpha^{-1}}{(b/\mu_m)(\mu_m \alpha^{-1} + (P_t - \theta y)/q)} \right) - yp(x), \\ G(x, y) &= e \min \left(x, \frac{Qx}{\theta} \right) p(x) - d. \end{aligned} \quad (3.7)$$

The nullclines of (3.2) are given by

$$\begin{aligned} \text{Producer nullclines: } & x[1 - \exp \{ F(x, y) \}] = 0, \text{ i.e., } x = 0 \text{ or } F(x, y) = 0, \\ \text{Grazer nullclines: } & y[1 - \exp \{ G(x, y) \}] = 0, \text{ i.e., } y = 0 \text{ or } G(x, y) = 0. \end{aligned}$$

The Jacobian of (3.2) is

$$J(x, y) = \begin{pmatrix} J_{11}(x, y) & x \exp \{ F(x, y) \} F_y(x, y) \\ y \exp \{ G(x, y) \} G_x(x, y) & J_{22}(x, y) \end{pmatrix}, \quad (3.8)$$

where

$$\begin{aligned}
F_x &= -b \max \left(\frac{1}{K}, \frac{1}{[b/\mu_m][\mu_m\alpha^{-1} + (P_t - \theta y)/q]} \right) - \left(\frac{f(x)}{x} \right)' y, \\
F_y &= \begin{cases} -p(x), & y < A(x), \\ -\frac{\mu_m\theta(x + \mu_m\alpha^{-1})}{q(\mu_m\alpha^{-1} + (P_t - \theta y)/q)^2} - p(x), & y > A(x), \end{cases} \\
G_x &= \begin{cases} e[p(x) + xp'(x)], & y < B(x), \\ \frac{e(P_t - \theta y + \mu_m q\alpha^{-1})}{\theta(\mu_m\alpha^{-1} + x)^2} (f'(x)(\mu_m\alpha^{-1} + x) - f(x)), & y > B(x), \end{cases} \\
G_y &= \begin{cases} 0, & y < B(x), \\ -\frac{x \cdot e \cdot p(x)}{\mu_m\alpha^{-1} + x}, & y > B(x), \end{cases} \\
J_{11}(x, y) &= \exp\{F(x, y)\} + x \exp\{F(x, y)\} F_x(x, y), \\
J_{22}(x, y) &= \exp\{G(x, y)\} + y \exp\{G(x, y)\} G_y(x, y).
\end{aligned} \tag{3.9}$$

To study the stability of the equilibria, we first introduce the standard Jury test (p57 of [4]).

LEMMA 3.1. *Let A be a 2×2 constant matrix. Both characteristic roots of A have magnitude less than 1 if and only if*

$$2 > 1 + \text{Det}(A) > |\text{Tr}(A)|.$$

Solving the system of algebraic equations

$$x[1 - \exp\{F(x, y)\}] = 0, \quad y[1 - \exp\{G(x, y)\}] = 0, \tag{3.10}$$

yields two boundary equilibria $E_0 = (0, 0)$ and $E_1 = (k, 0)$. At E_0 and E_1 , the Jacobians are

$$J(E_0) = \begin{pmatrix} \exp \left\{ b \left(1 - \frac{(\mu_m)^2 \alpha^{-1}}{b(\mu_m\alpha^{-1} + P_t/q)} \right) \right\} & 0 \\ 0 & e^{-d} \end{pmatrix}, \tag{3.11}$$

and

$$J(E_1) = \begin{pmatrix} 1 - b & kF_y(k, 0) \\ 0 & \exp\{G(k, 0)\} \end{pmatrix}, \tag{3.12}$$

respectively, where

$$G(k, 0) = e \min \left(k, \frac{Q}{\theta} k \right) p(k) - d.$$

By Lemma 3.1, we obtain the following theorem.

THEOREM 3.2. *For (3.2), E_0 is always unstable. E_1 is LAS if*

$$0 < b < 2 \text{ and } e \min \left(k, \frac{Q}{\theta} k \right) p(k) < d,$$

and it is unstable if

$$b > 2 \text{ or } e \min \left(k, \frac{Q}{\theta} k \right) p(k) > d.$$

Proof. The claim for E_0 is clear. If we let λ_1 and λ_2 be the characteristic roots of $J(E_1)$, then the condition

$$0 < b < 2 \text{ and } e \min \left(k, \frac{Q}{\theta} k \right) p(k) < d$$

ensures that $|\lambda_i| < 1, i = 1, 2$, while condition

$$b > 2 \text{ or } e \min(k, \frac{Q}{\theta}k)p(k) > d,$$

implies $\lambda_1 > 1$ or $\lambda_2 > 1$. ■

The fact that both (3.2) and (2.1) have the same equilibria suggests that (3.2) could have multiple equilibria. Now we assume that $E^* = (x^*, y^*)$ is such an equilibrium and discuss its local stability.

The Jacobian at the positive equilibrium (x^*, y^*) reads

$$J(E_*) = J(x^*, y^*) = \begin{pmatrix} 1 + x^*F_x & x^*F_y \\ y^*G_x & 1 + y^*G_y \end{pmatrix}, \quad (3.13)$$

where

$$F_x = F_x(x^*, y^*), F_y = F_y(x^*, y^*), G_x = G_x(x^*, y^*), G_y = G_y(x^*, y^*).$$

Its trace and determinant are

$$\text{Tr}(J(E_*)) = 2 + x^*F_x + y^*G_y, \quad (3.14)$$

$$\text{Det}(J(E_*)) = 1 + x^*F_x + y^*G_y + x^*y^*[F_xG_y - F_yG_x], \quad (3.15)$$

respectively. By carrying out arguments similar to those in Theorem 4.2 in [7], we obtain the following geometric statements on the locally asymptotic stability of the internal equilibrium E^* .

THEOREM 3.3. *In region Ω_1 ($y < P_t/\theta - (x + \mu_m/\alpha - q\mu_m/\alpha\theta)$), the following is valid. If the plant's nullcline is increasing at E^* (i.e., $F_x > 0$), then E^* is unstable. If the plant's nullcline is decreasing at E^* (i.e., $F_x < 0$) and*

$$\frac{1}{2}x^*y^*F_yG_x - 2 < x^*F_x < x^*y^*F_yG_x, \quad (3.16)$$

then E^ is LAS. If the plant's nullcline is decreasing at E^* (i.e., $F_x < 0$) and*

$$F_x > y^*F_yG_x \text{ or } x^*F_x < \frac{1}{2}x^*y^*F_yG_x - 2 \quad (3.17)$$

, then E^ is unstable.*

The following statements are true in region Ω_2 ($y > P_t/\theta - (x + \mu_m/\alpha - q\mu_m/\alpha\theta)$). If the slope of the plant's nullcline at E^ is greater than the herbivore's (i.e., $-G_x/G_y < -F_x/F_y$), then E^* is unstable. If the slope of the herbivore's nullcline at E^* is greater than the plant's (i.e., $-G_x/G_y > -F_x/F_y$) and*

$$\frac{1}{2}x^*y^*[F_yG_x - F_xG_y] - 2 < x^*F_x + y^*G_y < x^*y^*[F_yG_x - F_xG_y], \quad (3.18)$$

then E^ is LAS. If the slope of the grazer's nullcline at E^* is greater than the producer's (i.e., $-G_x/G_y > -F_x/F_y$) and one of the following inequalities holds,*

$$\begin{aligned} x^*F_x + y^*G_y &< \frac{1}{2}x^*y^*[F_yG_x - F_xG_y] - 2, \\ x^*F_x + y^*G_y &> x^*y^*[F_yG_x - F_xG_y], \end{aligned}$$

then E^ is unstable.*

TABLE 2. Parameter values used in simulation.

Parameter	Value	Unit
P_t	0.025	(mg P)/l
e	0.8	
b	1.2	day ⁻¹
d	0.25	day ⁻¹
θ	0.03	(mg P)/(mg C)
q	0.0038	(mg P)/(mg C)
c	0.81	day ⁻¹
a	0.25	(mg C)/l
μ_m	1.2	day ⁻¹
α	10.0	day ⁻¹
K	0.25-2.0	(mg C)/l

4. Numerical simulations. In this section, we provide numerical simulations for (2.1) and (3.2) to confirm and complement the analytical analysis. We choose the Monod-type function $f(x) = cx/(a+x)$ as the functional response of the herbivore. The parameter values listed in Table 2 are adapted from Andersen (1997) and Urabe & Sterner (1996). They are biologically realistic values. All the numerical simulations are done with MATLAB 7.0.

One can easily see that

$$(\ln f(x))'(\mu_m \alpha^{-1} + x) - 1 < 0$$

is satisfied with the initial conditions $x = 0.5$ (mgCl⁻¹), $y = 0.25$ (mgCl⁻¹). With this $f(x)$ and the parameters we have chosen, we have $G_x < 0$. This ensures stability changes when we vary light intensities.

In Figure1, for four different K values, we compare the dynamics of the KHE model (2.1) and the discrete KHE model (3.2). All solutions begin with the same initial conditions $x = 0.5$ (mgCl⁻¹), $y = 0.25$ (mgCl⁻¹).

First, we study the dynamics of the continuous KHE model (see Fig.1 (a1) (a2) (a3) (a4)). When $K = 0.25$, population densities stabilize around a stable equilibrium: $E^* = (x^*, y^*) = (0.16, 0.22)$ (see Fig.1 (a1)). When $K = 0.75$, population densities oscillate around an unstable equilibrium $E^* = (0.16, 0.48)$ (see Fig.1 (a2)). When $K = 1.0$, oscillatory solutions disappear and a stable equilibrium emerges with $x^* = 0.70, y^* = 0.42$ (see Fig.1 (a3)). When $K = 2$, the food is abundant, but the herbivore is driven to extinction due to low food quality: $E_1 = (2, 0)$ is the boundary equilibrium and $G(2, 0) < 0$, so E_1 is stable by Theorem 2.2. We can use the same ways to study the dynamics of the discrete KHE model by Theorem 3.2 and Theorem 3.3 (see Fig.1 (b1) (b2) (b3) (b4)). In Figure 1 (a1)-(a2) and (b1)-(b2), increasing K destabilizes the dynamics. This phenomenon is the Rosenzweig's paradox enrichment([21]). When K increases further, another positive equilibrium emerges (see Fig.1 (a3)-(b3)); although the plant density increases as K increases, its low quality (i.e., $P : C$) greatly constrains the herbivore's growth. This phenomenon is the paradox of energy enrichment ([16],[2]). In this situation, the herbivore-plant relationship is $(-, -)$ type. Finally, for large values of K (see

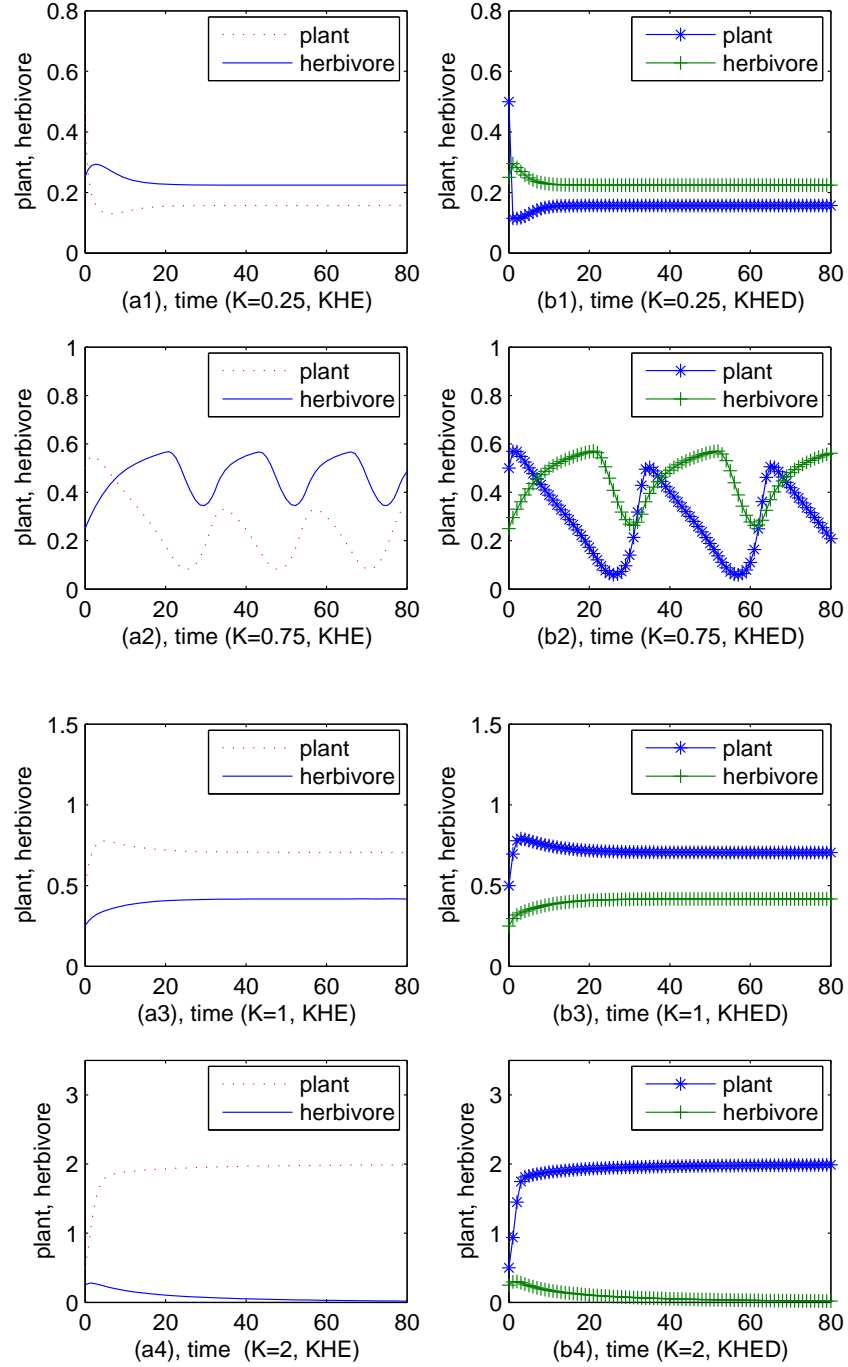


FIGURE 1. Here the parameters are defined in Table 1 and the initial conditions are $x = 0.5$ (mgCl^{-1}), $y = 0.25$ (mgCl^{-1}). (a_i) and (b_i) denote the dynamics of the KHE model (2.1) and the discrete KHE model (3.2) with different K , respectively.

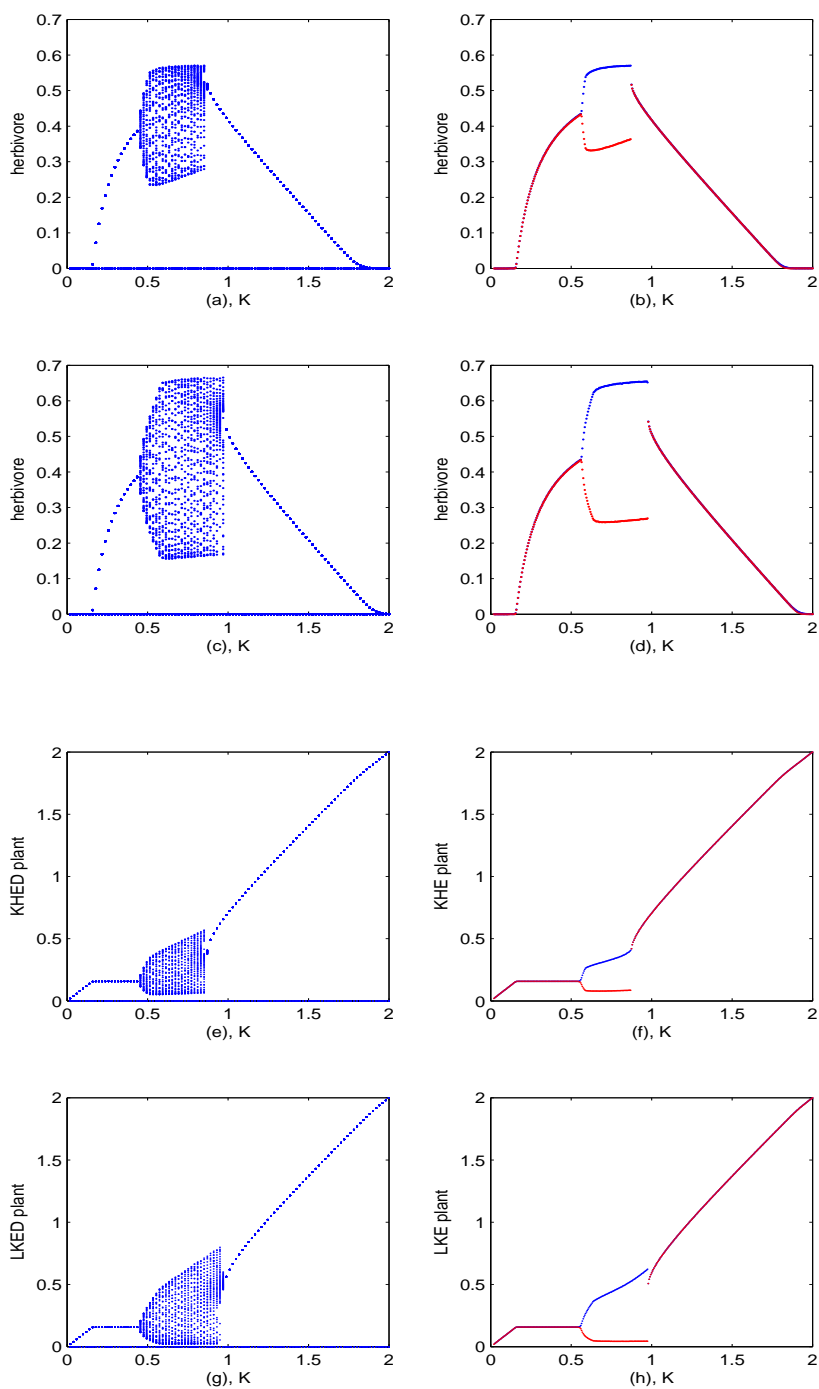


FIGURE 2. The bifurcation curves versus K for the discrete KHE model, the continuous KHE model, the discrete LKE model, and the continuous LKE model.

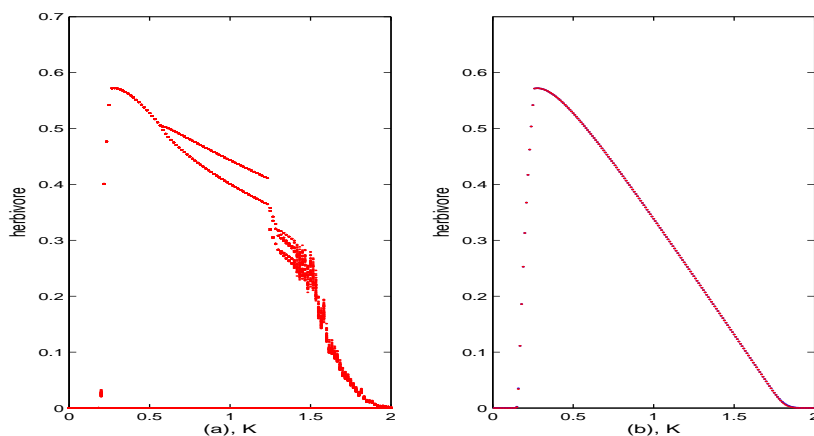


FIGURE 3. The bifurcation curves versus K for the discrete KHE model and the continuous KHE model, respectively. Here $b = 2.9$.

Fig. 1 (a4)-(b4)), the plant quantity is high, but its low quality drives the herbivore to extinction.

Figure 2 displays bifurcation curves with bifurcation parameter K for the discrete KHE and LKE models and for the continuous KHE and LKE models. When K is very small, the herbivore cannot survive because of starvation. As K increases, the herbivore persists at a stable equilibrium, and its density rises (see Fig. 2 (a) (b)). The herbivore-plant relationship is now a usual predator-prey (+, -) type (see Fig. 2 (a) (b) (e) (f)). As we further increase K , the stable equilibrium loses its stability through a Hopf bifurcation, and a limit cycle emerges. When K increases still further, the limit cycle disappears through an saddle-node bifurcation, and a new stable equilibrium emerges. Although the plant density increases as K increases (see Fig.2 (e) (f)), the herbivore's density decreases because of plant's low quality (see Fig.2 (a) (b)). The LKE model generates similar dynamics as the KHE model (see Fig.2 (c) (d) (g) (h)).

The numerical simulations in Figures 1 and 2 reveal that both the KHE model and its discrete analogue exhibit similar dynamics. But there are some notable differences. The amplitudes of the plant and herbivore densities in the discrete KHE model are larger than that of the continuous KHE model. The same holds for the LKE model and its discrete analogue. In addition, for both the KHE model and the LKE model, the internal equilibrium of the discrete systems loses its stability earlier than does that of the corresponding continuous models.

Moreover, the discretization can significantly affect the nature of attractors. For example, in Fig. 3, for the continuous model the global attractor is either the boundary equilibrium or the internal equilibrium (see Fig.3 (b)). However, for the corresponding discrete model (3.2) (see Fig.3 (a)), the global attractor can be a boundary equilibrium, an internal equilibrium, a limit cycle attractor, or even a strange attractor (chaos).

Figure 4 shows bifurcation diagrams for (3.2), (2.1), (3.3) and (3.5) against the intrinsic growth rate of the plant, b . Figure 4 (e) and (g) reveal the periodic doubling

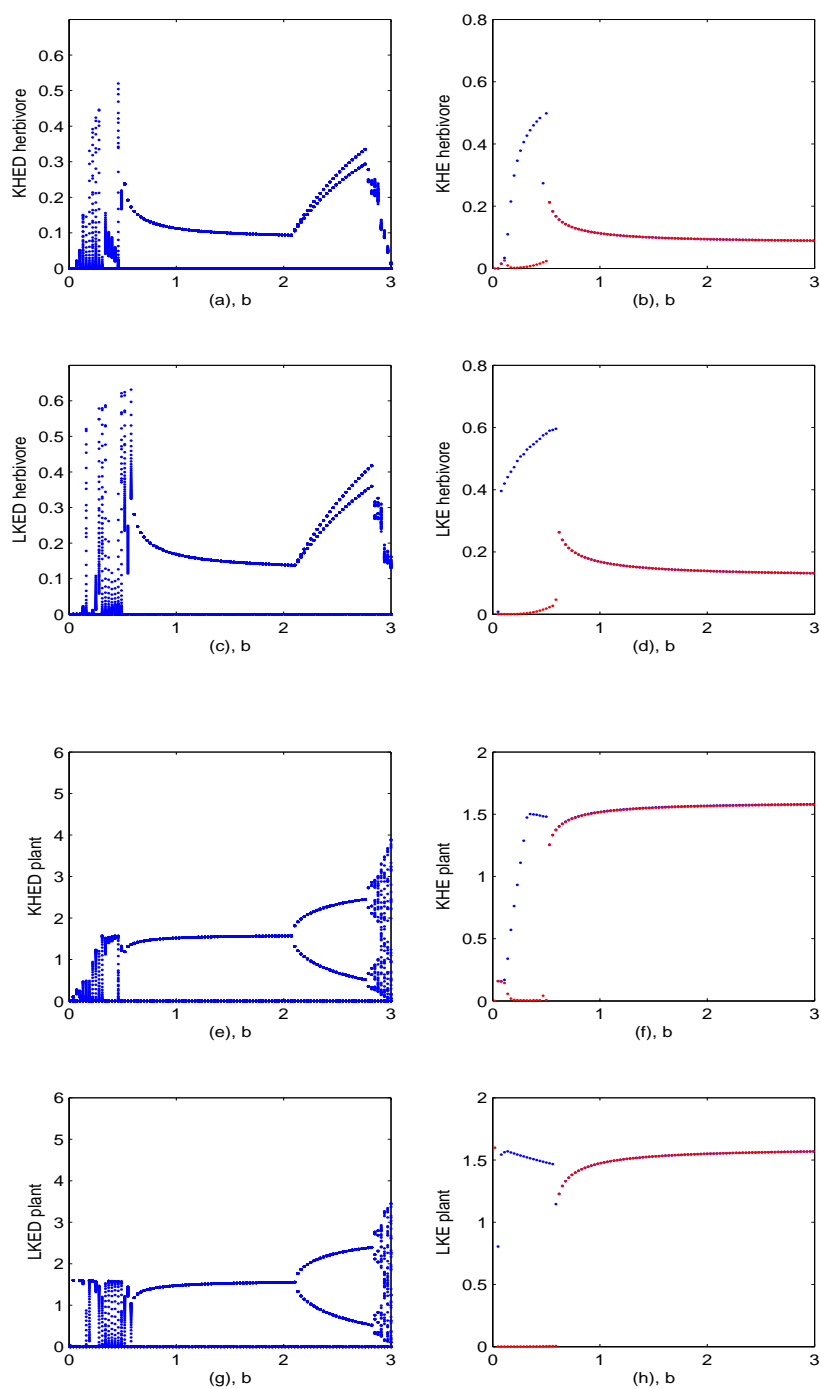


FIGURE 4. Bifurcation diagrams for the discrete KHE model, the continuous KHE model, the discrete LKE model, and the continuous LKE model, respectively. Here $K = 1.6$.

route to chaos for the plant's density, when b increases near 3. Interestingly, (a) and (c) in Figure 4 show that the herbivore's density quickly reaches zero shortly after the plant enters the chaos zone. This phenomenon shows that chaotic plant densities can be an important factor leading to the extinction of herbivores. But for the continuous KHE and LKE models, this biological conclusion is lost (see Fig.4 (b), (d), (f), (h)).

5. Discussion. The complexity of biological processes demands alternative, plausible models. A family of well-formulated models allows researchers to separate phenomena that are both robust and intrinsic to these processes, while recognizing those that are specific to a particular model structure. With this in mind, we have presented here a comparative study of four basic stoichiometric plant-herbivore models.

Although stoichiometric population models received increasing attention and support in the last decade (e.g., [1], [16], [18], [9], [13], [10]), almost all existing models have yet to be fully studied mathematically, and many can be modified or generalized to suit various new biological scenarios. All four models studied in this work have a main common feature: plant quality, expressed as C:P ratio, can vary and is determined by mass balance equations that track all P in the system. The distinct feature of the KHE model is that it allows free P in the system. In nutrient-limited pelagic systems, the concentration of free P is very low, making the LKE model appropriate. In terrestrial systems, the substantial soil compartment pool and delays in nutrient release cannot be ignored, and they demand explicit tracking of inorganic (free) P. In this sense, the KHE model can be viewed as a natural and important extension of the well-studied LKE model. To expand the applicability of the LKE and KHE models to non-overlapping generation dynamics, to annual plants, and to processes that are subject to periodic perturbations, it is desirable to study their discrete analogs.

Our analysis of the family of four models shows that stoichiometric effects of low food quality on herbivores are robust to discretization of time and addition of a free P pool. In all four models, poor plant quality is detrimental to herbivore growth, and, at its extreme, can drive herbivores to extinction. The reason is that prey with very low P:C, despite being a good source of calories, do not provide enough P to support the predator's growth. If prey quality is good (i.e., P:C is high), then these models behave like traditional energy-based predator-prey models such as Lotka-Volterra type models. All four stoichiometrically explicit models considered here show that an ever-increasing amplitude of the limit cycle is not the only possible scenario for enrichment of prey as suggested by the classical predator-prey models with Holling type II functional response ([21]). If the enrichment fuels the system with only one of the elements of which a plant is made, in our case C (e.g., via carbon dioxide fertilization or increase in incoming intensity of light), then the resulting low quality of the prey can halt oscillations and stabilize the system at an equilibrium with low grazer biomass (see Fig. 2); any further enrichment benefits the plant but leads to further decline in the grazer densities, a phenomena known as the paradox of energy enrichment ([16],[17],[2]). The models show that at different plant quality levels it is possible to have two (not simultaneous) equilibria: a high predator-prey ratio at high plant quality and low predator-prey ratio at low food plant quality. The existence of two such equilibria with strikingly different prey to predator ratios has been experimentally confirmed by Nelson et al. (2001)([19]).

While stoichiometric effects of low food quality are present in both continuous and discrete models, there are quantitative and qualitative effects that arise from discretization. Namely, the amplitude of the limit cycles is larger in discrete systems, and they are present at a larger range of parameter value, K . More important, the two discrete models reveal a possibility of chaotic dynamics and its role in the extinction of herbivores. As in Fan et al. [7], the discrete model shows that chaos can arise in a stoichiometric system because of variation in food quality. Andersen [1] was first to discuss such a possibility, and he provided some analysis in his higher-dimensional continuous model. Both discrete models clearly show a period-doubling route to chaos, which occurs within biologically plausible parameter ranges. This further supports Andersen's [1] argument on the possibility of chaos in stoichiometric systems.

Acknowledgments. We would like to thank the referees for their careful readings and their many suggestions that improved the presentation of this manuscript. The research of Meng Fan is supported in part by NSFC, the Key Project of the Ministry of Education, the sponsored project by SRF for ROCS, SEM. The research of Yang Kuang is supported in part by DMS-0436341 and DMS/NIGMS-0342388. Correspondence should be directed to Meng Fan.

REFERENCES

- [1] Andersen T., (1997). *Pelagic Nutrient Cycles: Herbivores as Sources and Sinks*, NY: Springer-Verlag.
- [2] Andersen T., J. J. Elser, and D. O. Hessen, (2004). Stoichiometry and population dynamics. *Ecol. Let.*, **7**, 884-900.
- [3] Droop, M. R., (1974). The nutrient status of algal cells in continuous culture. *J. Mar. Biol. Assoc. UK*, **55**, 825-855.
- [4] Edelman-Keshet L., (1988). *Mathematical Models in Biology*, McGraw-Hill.
- [5] Elser, J. J., R. W. Sterner, E. Gorokhova, W. F. Fagan, T. A. Markow, J. B. Cotner, J. F. Harrison, S. E. Hobbie, G. M. Odell, and L. J. Weider, (2000). Biological stoichiometry from genes to ecosystems. *Ecology Letters*, **3**, 540-550.
- [6] Elser, J. J. and J. Urabe, (1999). The stoichiometry of consumer-driven nutrient recycling: theory, observations, and consequences. *Ecology*, **80**, 735-751.
- [7] Fan, M., I. Loladze, Y. Kuang, J. J. Elser, (2005). Dynamics of a stoichiometric discrete producer-grazer model, *J. Difference Equations and Applications*, **11**, 347364.
- [8] Grover, J. P., (1997). *Resource Competition*, Chapman & Hall, London, UK.
- [9] Daufresne T. and M. Loreau, (2001). Ecological Stoichiometry, Primary Producer-Decomposer Interactions, and Ecosystem Persistence, *Ecology*, **82**, 3069-3082.
- [10] Hall S.R., (2004). Stoichiometrically Explicit Competition between Grazers: Species Replacement, Coexistence, and Priority Effects along Resource Supply Gradients, *Am. Nat.*, **164**, 157172.
- [11] Kuang, Y., J Huisman, J. J. Elser, (2004). Stoichiometric plant-herbivore models and their interpretation, *Math. Biosc. Eng.*, **1**, 215-222.
- [12] Lindroth, R.L., K.K. Kinney, and C.L. Platz. (1993). Responses of deciduous trees to elevated atmospheric CO₂: productivity, phytochemistry and insect performance, *Ecology*, **74**, 763-777.
- [13] Logan J. D., A. Joern, and W. Wolesensky, (2004). Control of CNP homeostasis in herbivore consumers through differential assimilation, *Bull. Math. Biol.*, **66**, 707-725.
- [14] Logan J. D., A. Joern, and W. Wolesensky, (2004a). Mathematical model of consumer homeostasis control in plant-herbivore dynamics, *Math. and Computer Modelling*, **40**, 447-456.

- [15] Loladze, I., (2002). Rising atmospheric CO₂ and human nutrition: toward globally imbalanced plant stoichiometry? *Trends in Ecology & Evolution*, **17**, 457-461.
- [16] Loladze I., Y. Kuang and J. J. Elser, (2000). Stoichiometry in producer-grazer systems: linking energy flow and element cycling, *Bull. Math. Biol.*, **62**, 1137-1162.
- [17] Loladze, I., Y. Kuang, J. J. Elser and W. F. Fagan, (2004). Coexistence of two predators on one prey mediated by stoichiometry, *Theor. Popul. Biol.*, **65**, 1-15.
- [18] Muller, E. B., R. M. Nisbet, S. A. L. M. Kooijman, J. J. Elser, and E. McCauley, (2001). Stoichiometric food quality and herbivore dynamics. *Ecol. Lett.*, **4**, 519-529.
- [19] Nelson, W. A., E. McCauley, and F. J. Wrona, (2001). Multiple dynamics in a single predator-prey system: experimental effects of food quality. *Proc. R. Soc. Lond. B.*, **268**, 1223-1230.
- [20] Newman, J. A., D. J. Gibson, E. Hickam, M. Lorenz, E. Adams, L. Bybee, and R. Thompson, (1999). Elevated carbon dioxide results in smaller populations of the bird cherry-oat aphid *Rhopalosiphum padi*, *Ecol. Entom.*, **24**, 486-489.
- [21] Rosenzweig, M. L., (1971). Paradox of enrichment: destabilization of exploitation ecosystems in ecological time. *Science*, **171**, 385-387.
- [22] Sterner, R. W. and J. J. Elser, (2002). *Ecological Stoichiometry*, Princeton University, Princeton, NJ.
- [23] Tilman, D., (1982). *Resource competition and community structure*, Princeton University Press, Princeton.
- [24] Urabe, J. and R. W. Sterner, (1996). Regulation of herbivore growth by the balance of light and nutrients. *Proceedings of the National Academy of Sciences, USA*, **93**, 8465-8469.
- [25] Urabe, J., J. J. Elser, M. Kyle, T. Sekino, and Z. Kawabata, (2002a). Herbivorous animals can mitigate unfavorable ratios of energy and material supplies by enhancing nutrient recycling. *Ecol. Lett.*, **5**, 177-185.
- [26] Urabe, J., J. Togari, and J. J. Elser, (2003). Stoichiometric impacts of increased carbon dioxide on planktonic herbivores. *Glob. Change Biol.*, **9**, 818-825.

Received on June 3, 2006. Accepted on July 2, 2006.

E-mail address: wtplay@hotmail.com

E-mail address: mfan@nenu.edu.cn

E-mail address: iloladze@math.unl.edu

E-mail address: kuang@asu.edu